Indian Journal of Science and Technology, *Vol 8(15), 51707, July 2015*
ISSN (Print) : 0974-6846
ISSN (Online) : 0974-5645

Studying the Effect of Indentation on Flow Parameters and Slow Heat Transfer of Water-Silver Nano-Fluid with Varying Volume Fraction in a Rectangular Two-Dimensional Micro Channel

Arash Karimipour[1], Habibollah Alipour[2], Omid Ali Akbari[2], Davood Toghraie Semiromi[2] and Mohammad Hemmat Esfe[1*]

[1]Department of Mechanical Engineering, Najafabad Branch, Islamic Azad University,Isfahan, Iran; m.hemmatesfe@gmail.com

[2]Department of Mechanical Engineering, Khomeinishahr Branch, Islamic Azad University, Khomeinishahr, Iran

Abstract

The purpose of this study is to investigate the influence of indentations on the parameters of fluid flow and heat of water-silver nanofluid in a rectangular two-dimensional micro channel. It includes heat transfer water silver nano fluid in an indented micro channel under the constant temperature. The system is numerically modeled, by Finite Volume Method. After solving the governing equations for U, V and θ, other useful quantities such as Nusselt number and friction factor can be determined. The hot fluid inlet exits after cooling by the cold walls of the micro channel. Calculations are done for the two ranges of Reynolds number (Re). It was observed that at times the fluid has more indentations; it has a greater temperature drop that is at the output cross section of the micro channel. With increasing Reynolds number (Re), number of the indentations and the increasing volume fraction of the nanoparticles, greater temperature drop occurs. The presence of indentation in the micro channel increases the speed and the dimensionless temperature at the center line. Finally, the results are provided in the form of the contour of flow and isothermal lines, the coefficient of friction, Nusselt number, temperature and velocity profiles in different micro channel sections. The results of the numerical simulation indicate that the heat transfer rate is significantly affected by the solid volume fraction and Reynolds number.

Keywords: Heat Transfer, Local Friction Factor, Nanofluid, Nusselt Number, Rib Micro Channel

1. Introduction

Improved heat transfer using new methods makes significant savings in energy costs and protecting the environment. Methods such as using suspensions instead of fluid factor in heat transfer equipment and the use of finned surfaces to enhance heat transfer surfaces and the use of sub-surfaces to disrupt laminar layer in the boundary layer of turbulent flow and to create secondary flows in order to better incorporate the flow factor in a heat transfer environment are the new techniques. The purpose of this study is to investigate the influence of indentations on the parameters of fluid flow and heat transfer of nanofluid in a rectangular two-dimensional micro channel. However, creating artificial teeth and ribbed surfaces in the direction of the fluid passing through the channel can significantly improve the heat transfer performance. But the added tooth will have unpleasant issues such as further pressure drop, creating areas with lower heat transfer on the back of the teeth, and higher pumping power to move fluid in the channel, in comparison with the smooth channel.

**Author for correspondence*

Many researchers investigated the flow behavior and heat transfer in channels and micro channels and Enclosure at different cross sections[1–8]. Much of this research focuses on examining the impact of parameters such as the Reynolds number, the channel cross-section, geometrical characteristics, arrangement of teeth, and attack angle of teeth and Type nanofluid[9–13]. Jung et al[14] experimentally investigated heat transfer in mandatory displacement of nano fluids in micro channels with water nano fluids - aluminum oxide and found that the coefficient of nano fluids displacement with volume ratio of 1/8% nano particles, more than 32 percent is higher than the rate of pure water displacement coefficient. In micro channels with smaller sizes, the heat transfer coefficient at comparable Reynolds numbers or larger than the coefficient of heat transfer in larger micro channels with higher Reynolds numbers, showing the micro channel heat transfer properties. Harris and colleagues[15] in an Experimental investigation of Water nano fluids - aluminum oxide concluded that the heat transfer coefficient increased turnover by 40 percent in comparison to pure water, while the thermal conductivity is increased up to 15 percent. Manka et al[16] studied the free displacement of heat transfer of nano fluids in a channel with teeth under constant heat flux. They concluded that the increasing Reynolds number and particle concentration both increase the average Nusselt number and the pressure drop. Han and colleagues[17] investigated the effects of tooth shape, angle of attack, and the ratio of step height on heat transfer. They concluded that with the same friction, the teeth with an angle of attack of 45° have a higher heat transfer performance than a tooth with 90°. Han and Park[18] studied the heat transfer in channels with different aspect ratios, and concluded that the channel with square cross section and a tooth with the angle of attack between 30° to 45° have the highest heat transfer performance. Jones and Emsit[19] examined the effect of height and spaces between teeth on heat transfer coefficient and concluded that the gap between the teeth is the most important geometrical parameter which can be considered as the characteristic length. Leo and Huang[20] examined the heat transfer performance of the fully developed flow in a channel with three square, semi-circular, and triangular teeth. They concluded that the above teeth have a comparable heat transfer performance and behind the square tooth compared to other areas, lower heat transfer areas are observed. Park et al[21] conducted empirical investigations in order to explain the friction in the turbulent flow and heat transfer behavior of nano fluids composed of Al_2O_3 and TiO_2 particles suspended in water in a circular pipe. They concluded that the increase in the volume concentration of nano particles increases the Nusselt number and there is a good relationship between Nusselt number and Reynolds number during the fully developed turbulent flow. Hove and colleagues[22] experimentally studied the effect of Tooth height on heat transfer in rectangular channels and found that increasing the blockage ratio (ratio of channel height to channel hydraulic diameter) improves the heat transfer. Leo and Huang[23] studied the numerical and experimental analysis of heat transfer and fluid flow behavior in rectangular channels with alternate arrangement of the teeth in the flow direction on one side of the main wall. They concluded that the speed and intensity of the turbulence are the important factors affecting the heat transfer coefficient. Wang and Sanden[24] in their empirical research to calculate the amount of local heat transfer in a square channel with teeth concluded that the local heat transfer rate is strongly dependent on the shape of the teeth. Rowe and colleagues[25] in their empirical research achieved the optimal step height and concluded that the increase in the rate of heat transfer not only depends on the aspect ratio of the teeth, but also depends on the shape of the teeth. Zhang and colleagues[26] in the study of heat transfer ratio in rectangular channels with grooved teeth found that creating grooves between the square teeth will not only increase the heat transfer rate but also decreases the pressure drop along the path. Han and colleagues[27] examined the transmission rate in a square channel for seven different angles (v-shaped) and concluded that the Chevron tooth with angle of 60° has heat transfer 4/5 times of the smooth channel and a better performance than the consistent teeth. Shen et al[28] experimentally investigated the flow and heat transfer in micro channel with rough walls with water fluid and concluded that the natural roughness has a very significant effect on the micro channel heat transfer in laminar flow and the coefficient of friction and the Nusselt number are significantly away from the classical theory. It is probably due to the roughness and the increased inflow temperature and power supply will promote the flow performance of heat.

2. Problem Statement

Figure 1 show the geometry used in this study that is a two-dimensional micro channel. Micro channel length is L = 2.5 mm and the hydraulic diameter is 2h = 50. The upper wall with the Length L and the bottom wall from the micro channel input and output sides are L/7. The central area of Micro channel is 5L/7 affected by temperature TC = 293. The Water inlet temperature of water-silver nano fluids is Th = 303° K, and the Water and Silver Nano particles are in thermal equilibrium.

Silver nano particles are spherical and uniform in shape and the micro channel flow is assumed slow, Newtonian, and incompressible under non-slip boundary condition at the walls and the Radiation effects are negligible. Thermo properties of pure water (base fluid) and silver nano particles at 298° K are shown in Table 1 and the water Prandtl number is Pr = 6.2. In this study, the study of fluids parameters and heat transfer have been performed with Reynolds numbers Re = 10 and the volume percentage of solid nano particles of 0, 0.02, 0.04 = φ. Table 1 shows Thermo physical properties of water, silver (Ag) and nanofluid[29].

At the present problem, in the micro channel Figure 1 we examine the effects of fluids parameters and heat transfer in the four states of D, C, B, A. In case (A) All calculations and analysis for micro channel of Figure 1 are performed and in case (B) the above parameters for micro channels of Figure 1 with respect to a tooth on the cold wall (below) with the length 7 L at the area 7 L/< X < 4 L/7 is investigated from the length of the input micro channel. In case (C), the calculation of parameters associated with each tooth length L/7 in the area of the micro channel (1) in the zone between 7 L/< X <3 7 L/2 and 7 L/< X <5 7 L/4 has been studied. In case (C) calculate the relevant parameters with two teeth along each L/7 in the area of micro form (1) regions between 7 L/<X <3 7 L/2 and 7 L/<X <5 7 L/4 has been investigated. In case (D) parameters calculated for the three teeth during each 7 L/ in the micro channel bottom wall (1) in the zone 5 2L/<X <7 L/ and 7 L/<X <5 7 L/4 and 7 L/6 <X <7 L/5 is investigated. For best results, all states in terms of form Figure 2 is shown. For all cases, D, C, B, A Tooth height is fixed and αH values of α = 0.1.

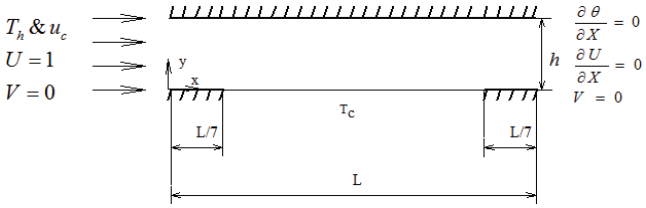

Figure 1. Schematic overview of the micro channel project areas A, B, C, D, is defined in.

3. Formulation

Dimensionless equations of governing equations include continuity, momentum and energy for steady-state in Cartesian coordinates[30].

$$\frac{\partial U}{\partial X}+\frac{\partial V}{\partial Y}=0 \tag{1}$$

$$U\frac{\partial U}{\partial X}+V\frac{\partial U}{\partial Y}=-\frac{\partial P}{\partial X}+\frac{\mu_{nf}}{\rho_{nf}\nu_f}\frac{1}{\mathrm{Re}}\left(\frac{\partial^2 U}{\partial X^2}+\frac{\partial^2 U}{\partial Y^2}\right) \tag{2}$$

$$U\frac{\partial V}{\partial X}+V\frac{\partial V}{\partial Y}=-\frac{\partial P}{\partial Y}+\frac{\mu_{nf}}{\rho_{nf}\nu_f}\frac{1}{\mathrm{Re}}\left(\frac{\partial^2 V}{\partial X^2}+\frac{\partial^2 V}{\partial Y^2}\right) \tag{3}$$

$$U\frac{\partial \theta}{\partial X}+V\frac{\partial \theta}{\partial Y}=\frac{\alpha_{nf}}{\alpha_f}\frac{1}{\mathrm{Re}\,\mathrm{Pr}}\left(\frac{\partial^2 \theta}{\partial X^2}+\frac{\partial^2 \theta}{\partial Y^2}\right) \tag{4}$$

In the above equations, the following dimensionless parameters are used,

$$X=\frac{x}{h}\qquad Y=\frac{y}{h}\qquad U=\frac{u}{u_c}\qquad V=\frac{v}{u_c}\qquad P=\frac{\overline{P}}{\rho_{nf}u_c^{\,2}}$$
$$\theta=\frac{T-T_c}{T_h-T_c}\qquad \mathrm{Re}=\frac{u_c h}{\upsilon_f}\qquad \mathrm{Pr}=\frac{\upsilon_f}{\alpha_f} \tag{5}$$

The following formula is used to calculate the density of nanofluids[30],

$$\rho_{nf}=(1-\varphi)\rho_f+\varphi\rho_s \tag{6}$$

Table 1. Thermo physical properties of water, silver (Ag) and nanofluid

Units	Water	Ag	Nanofluid φ=0.02	Nanofluid φ=0.04
c_p (J/kgK)	4179	235	3481.3	2976.2
ρ (kg/m³)	997	10,500	1187.2	1377.2
k (W/mK)	0.613	429	1.0052	1.4137
μ (Pa s)	8.91×10^{-4}	-	9.37×10^{-4}	9.86×10^{-4}

Brinkman equation is used for calculating the effective dynamic viscosity of nanofluids[31],

$$\mu_{nf} = \frac{\mu_f}{(1-\varphi)^{2.5}} \tag{7}$$

Nanofluids effective thermal diffusivity is calculated using the following formula[30],

$$\alpha_{nf} = \frac{k_{eff}}{(\rho C_p)_{nf}} \tag{8}$$

Nanofluid specific heat capacity is calculated with the following formula[30],

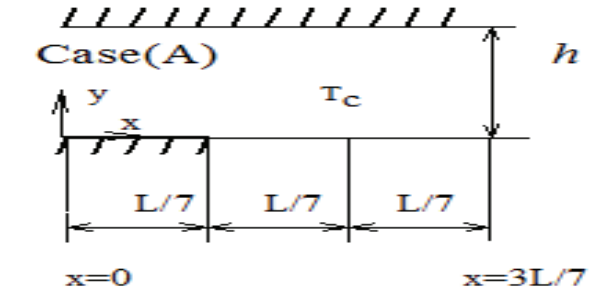

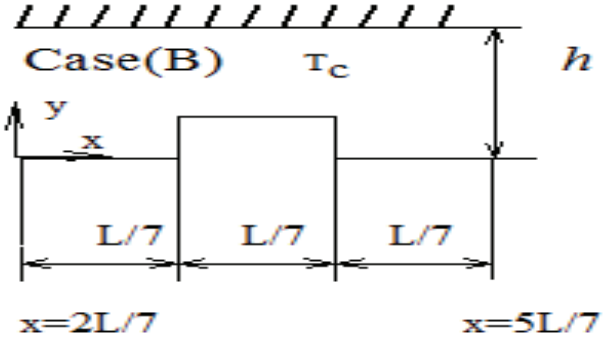

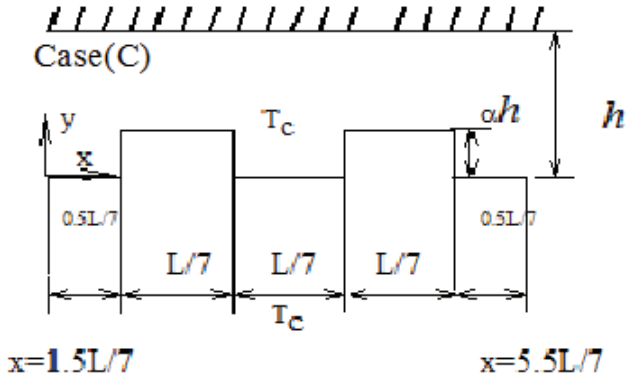

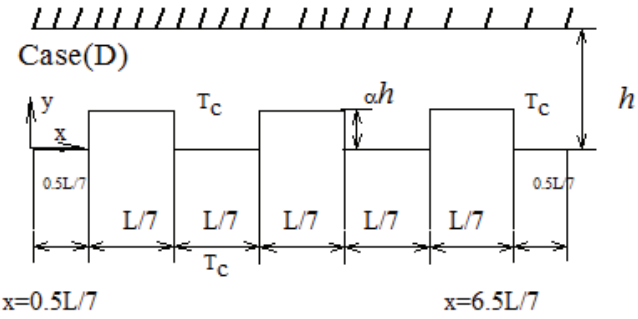

Figure 2. Schematic of Figures defined by A, B, C, D, show.

$$\left(\rho C_p\right)_{nf} = (1-\varphi)\left(\rho C_p\right)_f + \varphi\left(\rho C_p\right)_s \tag{9}$$

To calculate the effective thermal conductivity of nanofluids for suspension containing spherical particles Patel et al[32] equation is used:

$$k_{eff} = k_f\left[1 + \frac{k_s A_s}{k_f A_f} + ck_s Pe\frac{A_s}{k_f A_f}\right] \tag{10}$$

Empirical constant is c = 36,000

$$\frac{A_s}{A_f} = \frac{d_f}{d_s}\frac{\varphi}{1-\varphi} \tag{11}$$

$$Pe = \frac{u_s d_s}{\alpha_f} \tag{12}$$

In equations (11 and 12) the diameter of the water molecule is df = 2Å and the diameter of aluminum nano particles is equal to ds = 50nm. The speed us Brownian motion of nano particles is calculated using the following formula:

$$u_s = \frac{2\kappa_b T}{\pi\mu_f d_s^2} \tag{13}$$

In equation (13), the value of of $K_b = 1.3807\times10^{-23}$J/K bκ is Boltzmann's constant. To calculate the local Nusselt number along the bottom wall, we use the following equation,

$$Nu(X) = \frac{k_{eff}}{k_f}\left(\frac{\partial\theta}{\partial Y}\right)_{Y=0} \tag{14}$$

To calculate the local Nusselt number within the teeth width, we use the following equation:

$$Nu(Y)=\frac{k_{eff}}{k_f}\left(\frac{\partial\theta}{\partial X}\right)_{X=0} \quad (15)$$

To calculate the average Nusselt number along the horizontal portion of the lower wall, we use the following equation,

$$Nu_m|_X=\frac{1}{(L/7)}\int_{L/7}^{2L/7} Nu(X)dX \quad (16)$$

To calculate the average Nusselt number within any of the teeth we use the following equation,

$$Nu_m|_Y=\frac{1}{(\alpha_n H)}\int_0^{\alpha_n H} Nu(Y)dY;n=1,2 \quad (17)$$

The total Nusselt number on the surface of each tooth is equal to:

$$Nu_{m_{total}}=Nu_m|_X+Nu_m|_Y \quad (18)$$

$$C_f=\frac{\tau_w}{\frac{1}{2}\rho u_{ave}{}^2};\mu=\mu_f \,\&\, \rho=\rho_f \,\&\, u_{ave}=u_c \quad (19)$$

By replacing the Dimensionless parameters of part (5) in equation (19), (20) and (21) equations can be achieved

$$C_f(X)=\frac{2}{\mathrm{Re}}\left(\frac{\partial U}{\partial Y}\right)_{Y=0} \quad (20)$$

$$C_f(Y)=\frac{2}{\mathrm{Re}}\left(\frac{\partial V}{\partial X}\right)_{X=0} \quad (21)$$

To calculate the average friction coefficient along the horizontal portion of the lower wall, we use the following equation,

$$C_{fm}|_X=\frac{1}{(L/7)}\int_0^{L/7} C_f(X)dX \quad (22)$$

Flow lines have more changes with increasing Reynolds number in the area before and after the teeth. With the increase in the number of teeth, changes of flow lines are greater, because of the loss of fluid momentum due to the collision of the teeth. In lower Reynolds numbers these changes are less (i.e. for Reynolds Re = 10 flow line shifts towards Reynolds Re = 100 is less). For temperature lines after entering fluid at high temperature the following equation is used to calculate the average friction coefficient within the width of each tooth:

$$C_{fm}|_Y=\frac{1}{(\alpha_n H)}\int_0^{\alpha_n H} C_f(Y)dY;n=1,2 \quad (23)$$

The coefficient of local friction is equal to:

$$C_{fm_{total}}=C_{fm}|_X+C_{fm}|_Y \quad (24)$$

4. Results and Discussion

4.1 Examining the Reynolds Number and Nanoparticle Volume Fraction

This section examines the effects of Reynolds number Re = 10 and Re = 100 and nano particle volume fraction ($\varphi=0.04$) on flow lines and isothermal lines for all cases of A, B, C and D. Flow lines in Figures 3 to 6 show that, flow is developed after the arrival of flow to the micro channel. The development exists to the before hitting the teeth. After the encounter with the tooth, the flow is gone out of the development case. Discontinuities in the lower Reynolds and higher volume fraction of nano particles from heat transfer and the hot inlet increase to the cold inlet wall. Since the hot inlet fluid uses more time to deal with the mid-level at cold temperature, it can be seen that the fluid temperature drops more; it means that at the outlet micro channel with increasing Reynolds number, the number of teeth and the increasing volume fraction of nano particles, temperature drops more.

In Figure 7, the flow a is developed after going through the entrance area. This development will continue to hit the fluid to the teeth of the micro channel. With hitting

the teeth of micro channel, the speed increases and it is due to the shrinkage of micro channel for having no teeth and these changes are nearly constant with increasing the number of teeth. More changes in the dimensionless speed occur with increasing Reynolds number. Figure 8 shows the dimensionless temperature at the center of the micro channel for the cases A, B, C and D and the dimensionless temperature is closer to zero with increasing the number of teeth and reducing the Reynolds number in the output section. It means that more heat transfer occurs along the micro channel.

Figure 9 shows the graph for local Nusselt number along the dimensionless micro channel for cases A, B, C and D. It is observed that after hitting the fluid to the tooth due to the better mixing and more uniform temperatures in different layers of fluid, the Nusselt number increases suddenly over the micro channel. In the first teeth, the highest Nusselt number variations may occur. Nusselt number increases with the number of teeth, the volume fraction of nano particles and increasing Reynolds number.

Figure 10 shows the average Nusselt number in states A, B, C and D for the volume fraction of 0 to 0/4. It can be seen that the average Nusselt number at lower Reynolds with two teeth and different volume fraction has less changes. With more teeth and the volume fraction of nano particles, the Nusselt number increases. The effect of the presence of nano particles in higher Reynolds and higher volume fraction of nano particles s more pronounced at lower number of teeth. In Re = 100 it is observed that with increasing number of teeth and volume fraction of nano particles, average Nusselt number increases. However, we compare the average friction coefficient along the x and y for scenarios A, B, C and D with Reynolds number Re = 100, Re = 10 and φ = 0, 0.

Figure 11 shows the comparison of average Cf along

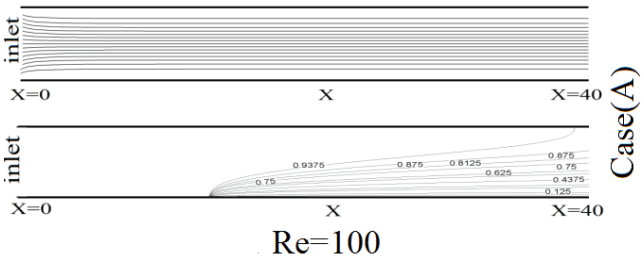

Figure 3. Graphs of flow lines and isotherms at Re = 10 and Re = 100 and Reynolds range of nanoparticle volume fraction (φ = 0.04) for the case (A).

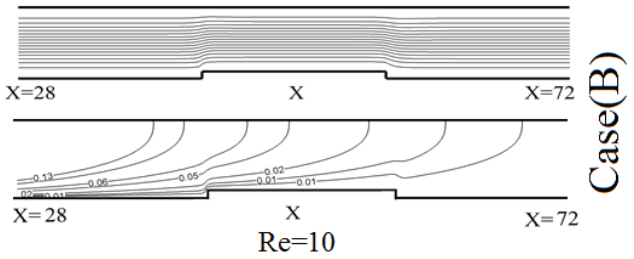

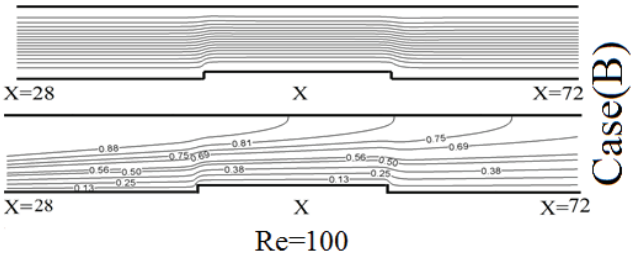

Figure 4. Graphs of flow lines and isotherms at Re = 10 and Re = 100 Reynolds range of nanoparticle volume fraction (φ = 0.04) for the case (B).

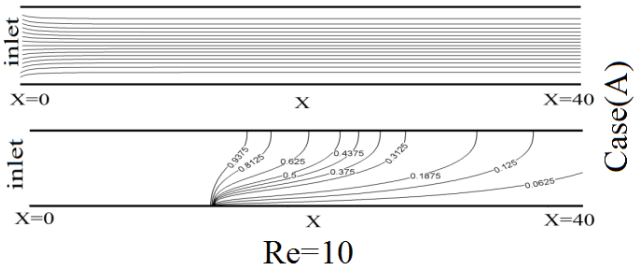

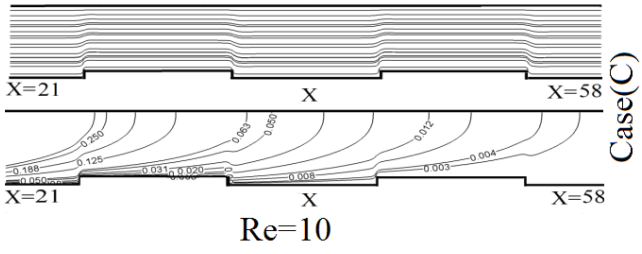

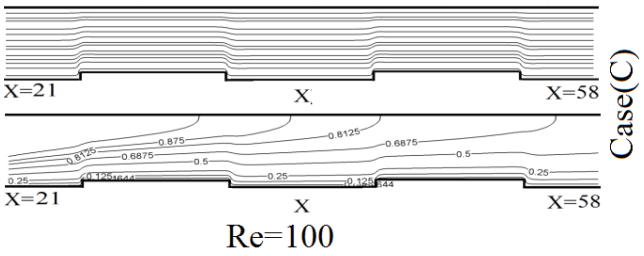

Figure 5. Graphs of flow lines and isotherms at Re = 10 and Re = 100 and Reynolds range of nanoparticle volume fraction (φ = 0.04) for the case (C).

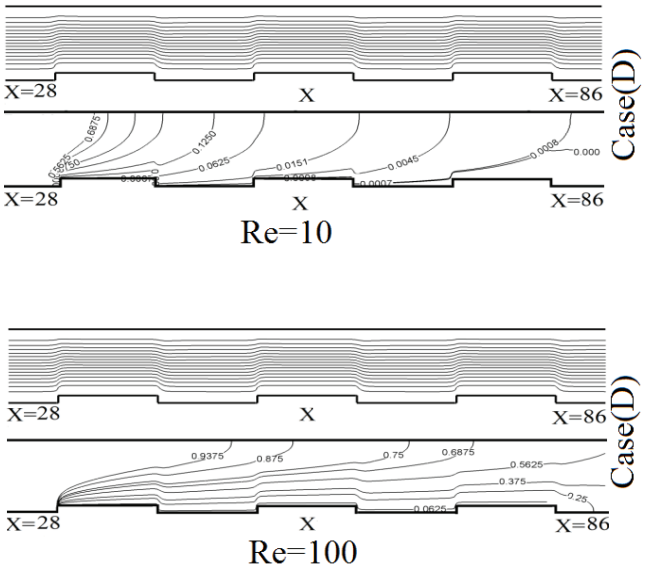

Figure 6. Graphs of flow lines and isotherms at Re = 10 and Re = 100 and Reynolds range of nanoparticle volume fraction (φ = 0.04) for the case (D).

the x and y for scenarios A, B, C and D. In high Reynolds the above average friction coefficient values along the x and y decreases, that is due to the collision to the teeth and decreased flow speed near the tooth. The friction coefficient increases with the number of teeth both along x and along y. increased number of teeth will cause more turbulence in the flow and more contact with the surface. In this section, we compare the friction coefficient Cf for Cases of D, B and Reynolds numbers Re = 10 and Re = 100 and φ = 0. In graphs of Figure 12 there is a sudden increase in the coefficient of friction such as the Nusselt number values for the coefficient of friction in areas with teeth. With decreasing Reynolds number, the fluid feels teeth more and the effects is transferred to the upper

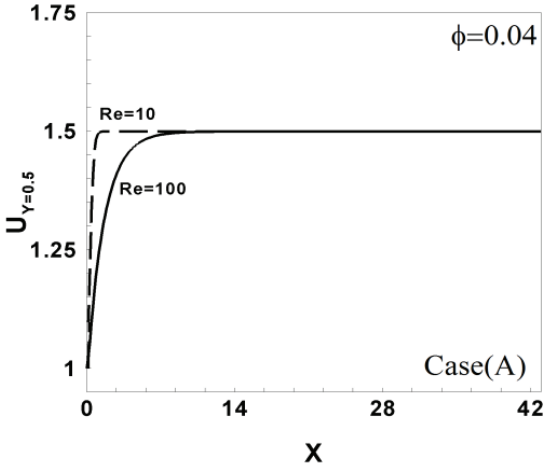

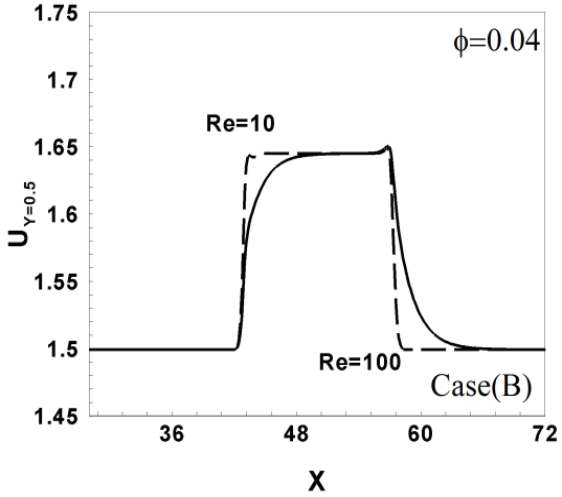

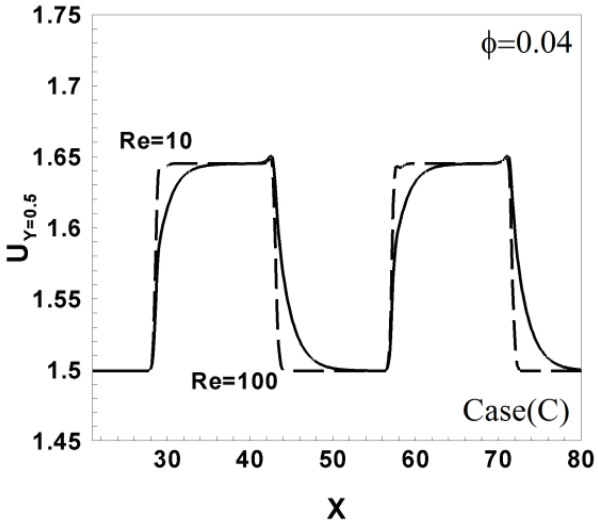

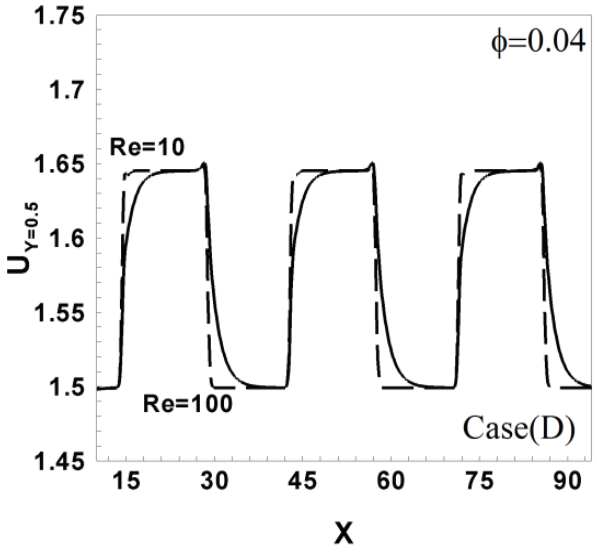

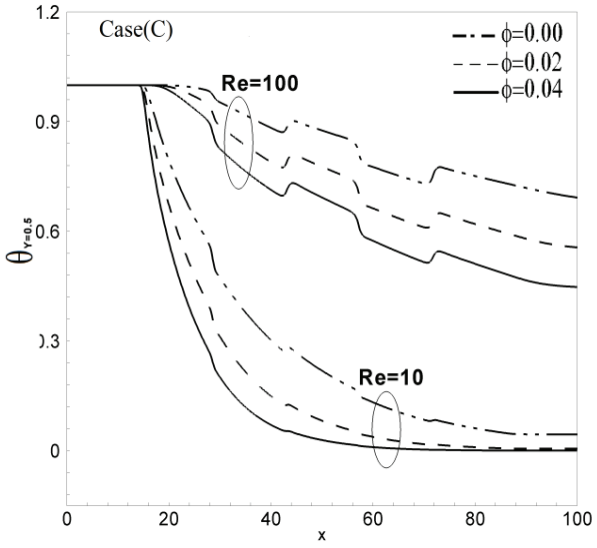

Figure 7. speeds at some point over the next micro channel four cases A, B, C, D.

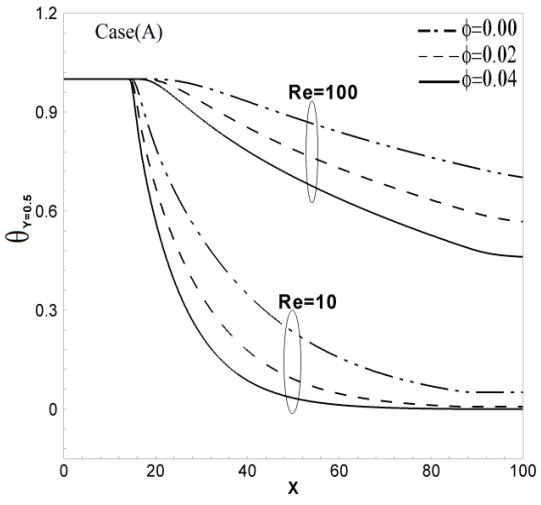

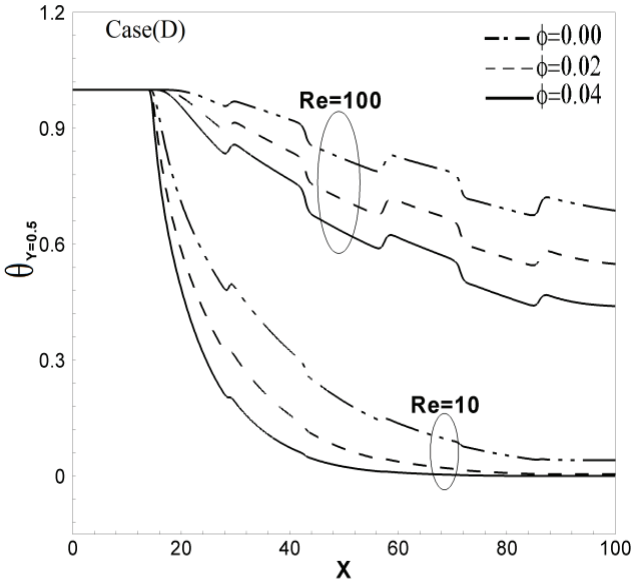

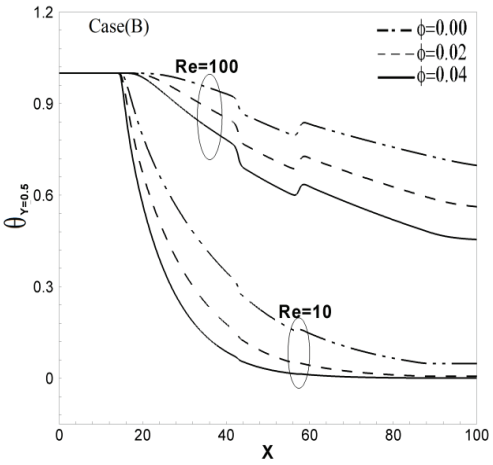

Figure 8. Temperature dimensionless micro channel Centre for case A, B, C, D.

layers of the fluid which increases the surface friction coefficient. The impact of the drop of transmission fluid velocity in the upper layer at Re = 100 ¬ less. Values of friction coefficient averaged along the axis (x) and (y) the Reynolds Re = 10 and Re = 100 and % v 0 = φ for scenarios A, B, C, D are precisely the values are given in Table 2.

The average friction coefficient increases with the increase of the number of teeth and reduced Reynolds number and it happens in horizontal walls and in line with the height of tooth in micro indentation occurs

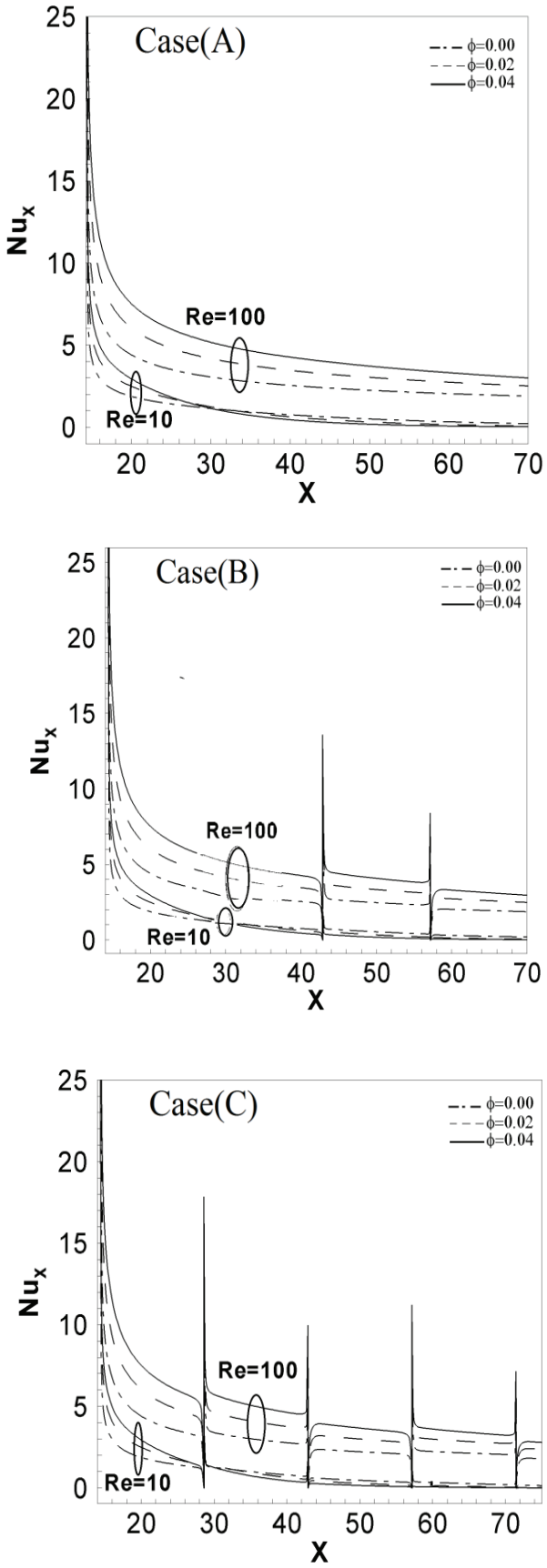

Figure 9. Graph of local Nusselt number along the dimensionless micro channel for cases A, B, C, D.

channel. It is mainly due to the increased number of teeth, which increases the contact surface between the wall and fluid. The other reason is due to the greater chance of passing the effects of tooth in the fluid layer near the wall in low Reynolds that increases the coefficient of friction.

Values of the average Nusselt number for the Reynolds are Re = 10 and Re = 100, and the volume percent φ =0, 0.02, 0.04 for scenarios A, B, C, D are given in Table 3. It is observed that increasing number of teeth and increasing

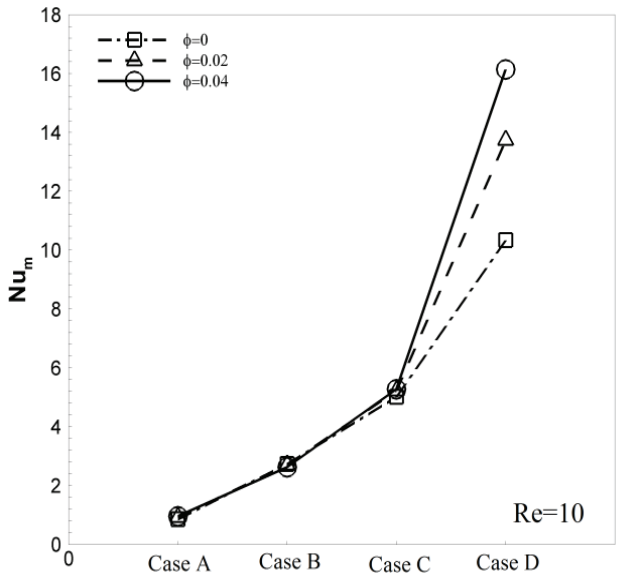

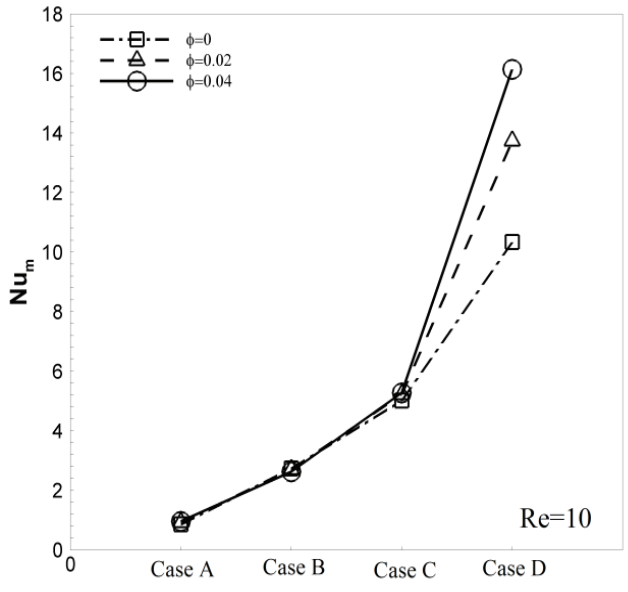

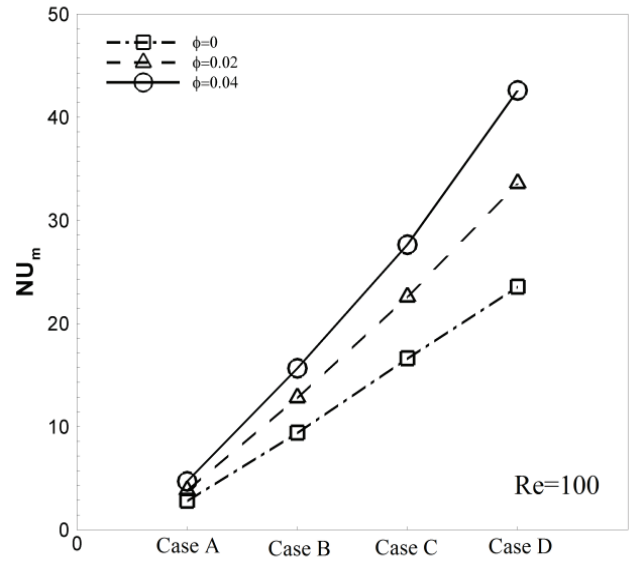

Figure 10. The average Nusselt number in cases A, B, C, D.

Reynolds number increase the average Nusselt number and this increase in heat transfer rate due to better mixing of the fluid layers near the surface is higher in Reynolds numbers due to teeth and strengthening the components of the fluid velocity. But on the other hand, with the significant increase in heat transfer due to the increase in the number of teeth increases the friction coefficient.

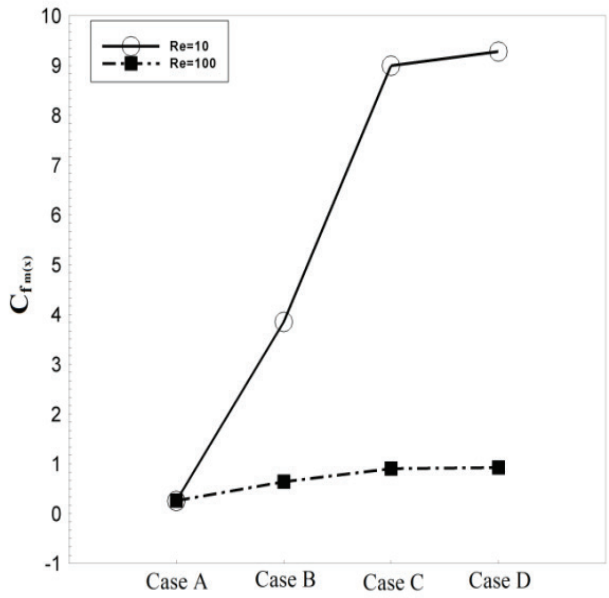

Figure 11. Comparison of mean C_f along the x and y for scenarios A, B, C, D.

5. Conclusion

With increasing volume fraction of the solid particles, the thermal performance of nano fluids increases owing to the volume of particles with relatively higher thermal conductivity. Significant increase in Nusselt number is more pronounced with increasing volume percent of solid particles, and an increase in the number of teeth caused by micro channels in high Reynolds. The presence of a tooth in the micro channel increases the speed and

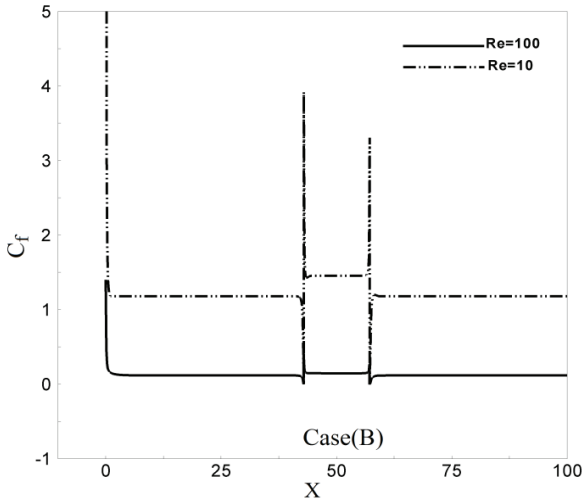

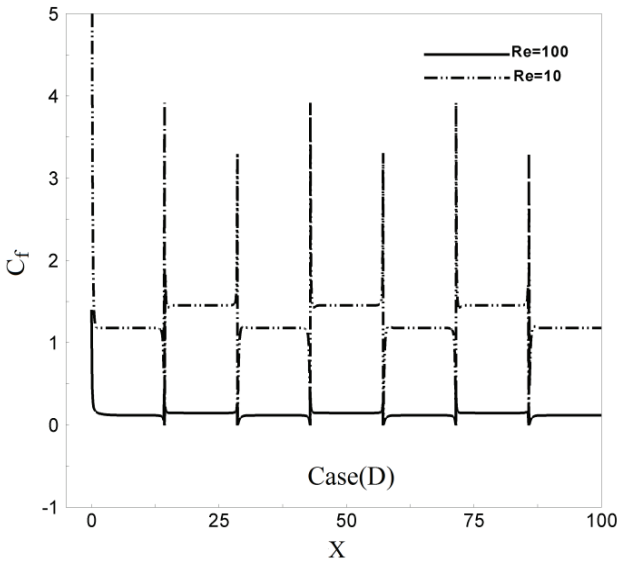

Figure 12. Comparison of friction factor C_f for the states of D, B and Reynolds numbers Re = 10 & Re = 100, and φ = 0,0.

Table 2. Different values $C_{fm}(x)$, $C_{fm}(y)$ for modes A, B, C, D the Reynolds number Re = 10 and Re = 100, and φ = 0,0

		$C_{fm}(x)$ (φ=0.00)	$C_{fm}(y)$ (φ =0.00)
Re = 10	Case (A)	0.2522	1.0216×10^{-8}
Re = 100		0.2601	6.7108×10^{-5}
Re = 10	Case (B)	3.8495	0.0831
Re = 100		0.6447	6.4029×10^{-3}
Re = 10	Case (C)	8.9949	0.1740
Re = 100		0.9032	0.0335
Re = 10	Case (D)	9.2751	0.6435
Re = 100		0.9292	0.0768

the dimensionless temperature of the central line.

Table 3. Different values Nu_m for modes A,B,C,D the Reynolds number Re=10 and Re=100 φ = 0,0.02,0.04

		Nu_m (φ=0.00)	Nu_m φ=0.02)	Nu_m φ=0.04)
Re=10	Case (A)	0.8673	0.9318	0.9644
Re=100		2.8146	3.8287	4.6834
Re=10	Case (B)	2.7452	2.7125	2.6236
Re=100		9.4297	12.8163	15.6655
Re=10	Case (C)	5.0180	5.2327	5.2728
Re=100		16.6163	22.6077	27.6377
Re=10	Case (D)	10.3473	13.7429	16.1369
Re=100		23.5645	33.6020	42.6044

6. References

1. Karimipour A, Esfe MH, Safaei MR, Semiromi DT, Jafari S, Kazi SN. Mixed convection of copper-water nano fluid in a shallow inclined lid driven cavity using the lattice Boltzmann method. Physica A. 2014; 402:150–68.
2. Goodarzi M, Safaei MR, Oztop HF, Karimipour A, Sadeghinezhad E, Dahari M, Kazi SN, Jomhari N. Numerical study of entropy generation due to coupled laminar and turbulent mixed convection and thermal radiation in an enclosure filled with a semitransparent medium. Scientific World Journal. 2014; 8.
3. Karimipour A, Nezhad AH, Behzadmehr A, Alikhani S, Abedini E. Periodic mixed convection of a nano fluid in a cavity with top lid sinusoidal motion. Proceedings of IMechE Part C. J. Mech. Eng. Sci. 2011; 225. :2149–60.
4. Karimipour A, Mirtalebi SS, Afrand M. Using nano fluid in lid driven shallow enclosure at particular Richardson number: investigation the effect of velocity ratio. Indian Journal of Science and Technology. 2014 May; 7(5):698–04.
5. Ahmed S. The effect of viscous dissipative heat on three dimensional oscillatory flow with periodic suction velocity. Indian Journal of Science and Technology. 2010 Mar; 3(3):276–83.
6. Pradeep JSE, Shree Meenakshi K. Synthesis of silver nano fluid by a novel one pot method for heat transfer applications. Indian Journal of Science and Technology. 2011 Apr; 4(4):417.
7. Atefi R, Khajeali M, Rasafchi M. Effect of multi-wall carbon nano tubes with different volume fractions on surface roughness in electro discharge machining. Indian Journal of Science and Technology. 2014 May; 7(5):648–53.
8. Kalbasi M, Saeedi AR. Numerical investigation into the convective heat transfer of CuO nano fluids flowing through a straight tube with uniform heat flux. Indian Journal of Science and Technology. 2012 Mar; 5(S3):2455–8.
9. Karimipour A, Nezhad AH, D'Orazio A, Shirani E. The effects of inclination angle and Prandtl number on the mixed convection in the inclined lid driven cavity using Lattice Boltzmann method. J Theor App Mech. 2013; 51(2): 447–62.
10. Karimipour A, Nezhad AH, D'Orazio A, Shirani E. Investigation of the gravity effects on the mixed convection heat transfer in a microchannel using lattice Boltzmann method. Int J Therm Sci. 2012; 54:142–52.
11. Pawar CB, Aharwal KR, Chaube A. Heat transfer and fluid flow characteristics of rib-groove roughened solar air heater ducts. Indian Journal of Science and Technology. 2009 Nov;

2(11): 50–4.
12. Esfe MH, Akbari M, Toghraie D, Karimipour A, Afrand M. Effect of nano fluid variable properties on mixed convection flow and heat transfer in an inclined two-sided lid-driven cavity with sinusoidal heating on sidewalls. Heat Trans. Res. 2014; 45:409–32.
13. Esfe MH, Arani AAA, Karimipour A, Esforjani SSM. Numerical simulation of natural convection around an obstacle placed in an enclosure filled with different types of nano fluids. Heat Trans Res. 2014; 45:279–92.
14. Jung JY, Oh HS, Kwak HY. Forced convective heat transfer of nano fluids in micro channels. Int J Heat Mass Transfer. 2009; 52:466–72.
15. Heris SZ, Etemad SGh, Esfahany MN. Experimental investigation of oxide nano fluids laminar flow convective heat transfer. International Communication in Heat and Mass Transfer. 2006; 33: 529–35.
16. Manca O, Nardini S, Ricci D. A numerical study of nano fluid forced convection in ribbed channels. Applied Thermal Engineering. 2012; 37: 280-92.
17. Han JC, Glicksman LR, Rohsenow WM. An investigation of heat transfer and friction for rib-roughened surfaces. Int J Heat Mass Transfer. 1978; 21(7): 1143–56.
18. Han JC, Park JS. Developing heat transfer in rectangular channels with rib taurbulators. Int J Heat Mass Transfer. 1988; 31(1):183–95.
19. Jones CD, Smith LF. Optimum arrangement of rectangular fins on horizontal surfaces for free convection heat transfer. J Heat Trans Trans. ASME Ser. 1970; C 92:6–10.
20. Liou TM, Hwang JJ. Effect of ridge shapes on turbulent heat transfer and friction in rectangular channel. Int J Heat Mass Transfer. 1993; 36(4):931–40.
21. Park BC, Cho YI. Hydrodynamic and heat transfer study of dispersed fluids with submicron metallic oxide particles. Exp Heat Transf. 1998; 11:151–70.
22. Huh M, Liu YH, Han JCh. Effect of rib height on heat transfer in a two pass rectangular channel (AR = 14) with a sharp entrance at high rotation numbers. Int J Heat Mass Transfer. 2009; 52:4635–49.
23. Liou TM, Hwang JJ, Chen SH. Simulation and measurement of enhanced turbulent heat transfer in a channel with periodic ribs on one principal wall. Int J Heat Mass Transf. 1993; 36:507–17.
24. Wang L, Sunden B. Experimental investigation of local heat transfer in a square duct with various-shaped ribs. Int J Heat Mass Transf. 2006; 43:759–66.
25. Rau G, Cakan M, Moeller D, Arts T. The effect of periodic ribs on the local aerodynamic and heat transfer performance of a straight cooling channel. J Turbomach. 1998; 120:368–75.
26. Zhang YM, Gu WZ, Han JC. Heat transfer and friction in rectangular channel with ribbed or ribbed-grooved walls. ASME/J. Heat Transfer. 1994; 116:58–65.
27. Han JC, Zhang YM. High performance heat transfer ducts with parallel broken and V-shaped broken ribs. International Journal of Heat and Mass Transfer. 1992; 35:513–23.
28. Shen S, Xu JL, Zhou JJ, Chen Y. Flow and heat transfer in micro channels with rough wall surface. Energy Convers. Manag. 2006; 47:1311–25.
29. Mahdy A. Unsteady mixed convection boundary layer flow and heat transfer of nano fluids due to stretching sheet. Nuclear Engineering and Design. 2012; 249:248–55.
30. Aminossadati SM, Ghasemi B. Natural convection cooling of a localized heat source at the bottom of a nano fluid-filled enclosure. European Journal of Mechanics B/Fluids. 2009; 28:630–40.
31. Brinkman HC. The viscosity of concentrated suspensions and solution. J Chem Phys. 1952; 20:571–81.
32. Patel HE, Sundararajan T, Pradeep T, Dasgupta A, Dasgupta N, Das S KA. Micro-convection cassel for thermal conductivity of nano fluids. Pramana J Phys. 2005; 65(5):863-69.

Appendix

Nomenclature

A	Area, m^2
c	Experimental constant, Equation (10)
C_f	friction factor
C_p	Heat capacity, $Jkg^{-1}K^{-1}$
d	Diameter, nm
g	Gravity acceleration, ms^{-2}
h, l	Microchannel height and length, m
H = h/h, L = l/h	Dimensionless microchannel height and length
k	Thermal conductivity coefficient, $Wm^{-1}K^{-1}$
Nu_X, Nu_m	Local and averaged Nusselt number
p	Fluid pressure, Pa
$\bar{p}$	Modified pressure, Pa
$P = (\bar{p} / \rho_{nf} u_c^2)$	Dimensionless pressure
$Pe = (u_s d_s / \alpha_f)$	Peclet number
$Pr = \upsilon_f / \alpha_f$	Prandtl number
$Re = \rho_f u_c h / \mu_f$	Reynolds number
T_H, T_C	Hot and cold Temperature, K
u,v	Velocity components in x , y directions, ms^{-1}
uc	nlet flow velocity, ms^{-1}
u_s	Brownian motion velocity, ms^{-1}
$(U,V) = (u/U_0, v/U_0)$	Dimensionless flow velocity in x-y direction
x,y	Cartesian coordinates, m
(X,Y) = (x/h,y/h)	Dimensionless coordinates

Greek symbols

α	Thermal diffusivity, m^2s^{-1}

φ	Nano particles volume fraction	c	Cold
κ_b	Boltzmann constant, JK^{-1}	f	Base fluid (pure water)
μ	Dynamic viscosity, Pas	h	Hot
$\theta = (T-T_C)/(T_H-T_C)$	Dimensionless temperature	m	mean
ρ	Density, kgm^{-3}	nf	Nano fluid
υ	Kinematics viscosity, m^2s^{-1}	s	Solid nano particles

Super- and Sub-scripts